Vehicle-track-soil interaction and train-induced ground vibration – Theory and measurements in Germany, Switzerland and France

IOP Conf. Series: Journal of Physics: Conf. Series **1264** (2019) 012034 doi:10.1088/1742-6596/1264/1/012034

Vehicle-track-soil interaction and train-induced ground vibration – Theory and measurements in Germany, Switzerland and France

L Auersch

Federal Institute of Material Research and Testing, 12200 Berlin, Germany

Lutz.auersch-saworski@bam.de

Abstract. Three measurement campaigns of train-induced ground vibrations are evaluated for the vehicle-track-soil interaction. Ground vibrations, track vibrations and vehicle vibrations have been measured for train passages and impulse excitation and compared with theoretical results. The soil and the track-soil system are calculated by wavenumber integrals. The influence of the vehicle is introduced by a substructure method. By comparing theory and measurement the different components of excitation force and ground vibration can be analysed, the quasi-static excitation, track-alignment errors, the out-of-roundness of wheels, the wheel and rail roughness, and moreover, scattered axle impulses and ineffective high-frequency parts of the wheelset accelerations and forces.

1. Introduction

Vehicle-track interaction has been analysed without any soil model or with very simple soil models in the past e.g. [1,2]. More rigorous continuous soil models have been introduced in the analysis mainly in the last twenty years e.g. [3-7]. Experimental ground vibration studies, on the other hand, are restricted to the soil sub-system in most cases e.g. [8-10]. The aim of the present contribution is to cover the whole vehicle-track-soil interaction and the induced ground vibration. It is the result of the cooperation with the German Railways (DB), the Swiss Railways (SBB) and the École Centrale de Nantes. In each country, a measurement campaign has been performed where the measurement of the ground vibrations has been combined with measurements of the vehicle vibration and the track irregularities. The central part of each campaign will be presented, the transfer function and the train-induced vibration of the soil and the wheelset accelerations with the estimation of the irregularities and the excitation forces.

The contribution starts with some methods for the track-soil and the vehicle-track interaction. Then the three measurement campaigns and their main results are presented in the order Germany, Switzerland and France. Finally, the consequences from the comparisons are discussed including some further literature.

2. Methods of vehicle-track-soil interaction

2.1. The ground vibration and the track-soil interaction

The behaviour of the soil and the track-soil system is calculated in the frequency-wavenumber domain. The response of a homogeneous or layered soil in frequency-wavenumber (ξ,f) domain can be calculated

by different matrix methods [11-13]. The admittance $H_S(\xi,f)$ for a plane stress wave excitation can be integrated to get the particle velocity v_P at distance r of a point load F

$$v_P(r,f) = \frac{F}{2\pi}\int_0^\infty H_S(\xi,f)J_0(\xi r)\mathrm{d}\xi$$

where J_0 is the Bessel function. A constant rectangular load has been used as an approximate train load. The wavenumber transforms of the uniform force distribution along and across the track

$$p_1(\xi_x) = \frac{\sin\xi_x a/2}{\xi_x a/2} \qquad p_2(\xi_y) = \frac{\sin\xi_y b/2}{\xi_y b/2}$$

have been introduced in the double wavenumber integral

$$v_T(x,y,f) = \frac{F}{2\pi}\int_{-\infty}^{+\infty}\int_{-\infty}^{+\infty} H_S(\xi_x,\xi_y,f)p_1(\xi_x)p_2(\xi_y)\exp \mathrm{i}(\xi_x \mathrm{x} + \xi_y \mathrm{y})\,\mathrm{d}\xi_x \mathrm{d}\xi_y$$

The ratio between the track- and point-load solution has been evaluated for homogeneous soils in Figure 1. The shear wave velocity has been varied between realistic 100 and 300 m/s while the mass density and the Poisson's ratio are kept constant at 2000 kg/m and 0.33. The rectangular track-like excitation yields smaller amplitudes, smaller for slower wave velocity and for higher frequencies. The reduction starts well in the range of train induced ground vibrations between 10 and 100 Hz.

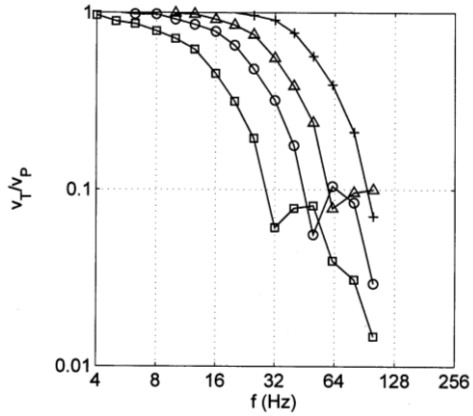

Figure 1. Ratio between the soil response to a track load (width b = 2.6 m) and a point load for different soils with shear wave velocity v_S = □ 100,○ 150, △ 200, and + 300 m/s.

2.2. The vehicle-track interaction for irregularity excitation

In most of the recent analyses, e.g. [4-7], the irregularity is understood as the main excitation of the ground vibration. The irregularities of vehicle and track produce accelerations of the passing vehicle and corresponding excitation forces. The analysis of vehicle models show that the car body is decoupled from the rest above 1 or 2 Hz. The bogie has some amplified vibrations around 10 Hz, but the mass is not so big. Finally, there is a wide frequency range where the mass m_W and the acceleration a of the wheelset are the dominating source of the excitation forces.

The model of the vehicle or the wheelset (the frequency-dependent vehicle stiffness $K_V = F/u_W$) can be coupled to the track-soil model (the frequency-dependent track-soil stiffness $K_T = F/u_T$) as

$$H_{VT}(f) = \frac{F}{s}(f) = \frac{K_V(f)K_T(f)}{K_V(f)+K_T(f)}$$

to get the vehicle-track transfer function $H_{VT}(f)$ between the irregularity s and the excitation force F [14]. This transfer function starts at low frequency strongly increasing as $H_{VT}(f) \approx K_V(f) \approx -m_W(2\pi f)^2$, has a vehicle-track resonance and is rather constant $H_{VT}(f) \approx K_T(f)$ at higher frequencies.

3. Measurements at the German site with train speed variation

3.1. Overview on the vehicle, track and ground measurements

The measurement site is located near Würzburg near a high-speed line [15]. A test train consisting of an engine, five passenger cars and another engine was running at speeds between 16 and 160 km/h [16].

The results for the vehicle (measured with accelerometers), track and ground (measured with geophones on spikes) are shown in Figure 2 for the normal train speed of 160 km/h. The car body has the lowest acceleration of the vehicle whereas the bogie and the wheelset accelerations are almost the same (Fig. 2a). Above 32 Hz, the wheelset accelerations are clearly the highest. The velocity amplitudes of the track are almost constant for all frequencies (Fig. 2b). There are three third octave bands around 16 Hz with raised amplitudes, but they do not correlate with the three raised amplitudes of the vehicle around 8 Hz. Finally, the velocity amplitudes of the ground vibration are presented for different distances to the track in Figure 2c. The amplitudes attenuate with distance and a general pattern can be found. The nearest point has rather constant spectra whereas all other points show dominating frequency ranges around 12 and 50 Hz. Lower and higher frequencies are clearly reduced due to layering and damping.

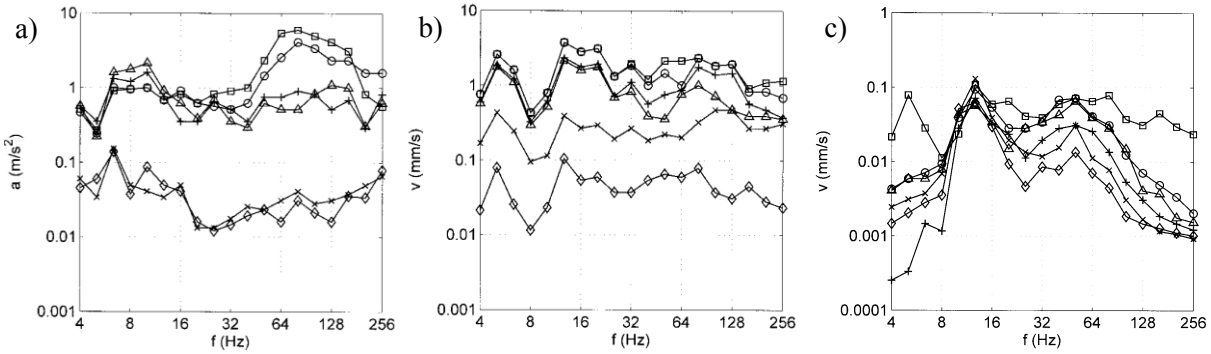

Figure 2. German test site, train speed v_T = 160 km/h, a) vehicle accelerations □,○ wheel 1 and 2, △,+ bogie 1 and 2, ×,◇ car body 1 and 2, b) track velocities □ rail 1 (between),○ rail 2 (on sleeper), △,+ sleeper 1 and 2, × sleeper horizontal, ◇ soil at 2.5 m, c) ground particle velocities at □ 2.5, ○ 7.5, △ 12.5, + 20, × 30, ◇ 50 m.

3.2. Vehicle vibrations for different train speeds

The accelerations of different vehicle points are presented in Figure 3 for different train speeds. The amplitudes of the car body are small for all train speeds (Fig. 3a). The amplitudes of the bogie are greater (Fig. 3b), but still smaller than the high-frequency wheelset amplitudes. Two wheels of a bogie are presented in Figures 3c,d. The low-frequency amplitudes are very similar so that in can be concluded that all wheels are passing over the same track irregularities (track alignment errors). Some variation can be observed for the first wheel out-of-roundness at 8 to 16 Hz (Fig. 3d). At low frequencies, the wheelsets follow the irregularities so that $a \sim s(2\pi f)^2$. The constant accelerations a would mean an irregularity that is decreasing as $s \sim f^{-2}$. The wheel accelerations start to increase between 12 and 32 Hz and reach the highest level above 50 Hz. The high-frequency amplitudes are due to the vehicle-track or the wheelset-track resonance where the wheelset mass is vibrating on the compliance of the track. This resonance is clearly seen on a slab track at 64 Hz (Fig. 3f) because of the soft rail pads which have only little material damping and which prevent the radiation damping into the soil. The ballast track has a stronger damping and a weaker and wider resonance (Fig. 3c). In the same frequeny region, speed-dependent peaks of the wheel accelerations can be found (Fig. 3d). The peaks at 32, 40, 50, 63 and 80 Hz correlate with the train speed in frequency $f \sim v_T$ and in amplitude $A \sim v_T^2$. They are strongest for the ballast track on a bridge (Fig. 3e). These peaks are due to the passage over the equally spaced sleepers.

3.3. Ground vibration measurements for hammer and train excitation

Hammer impacts have been applied to the soil and the response of the soil has been evaluated to estimate wave velocities and transfer functions [17]. The measured transfer functions in Figure 4a have been approximated by a layered soil model (Fig. 4b). The wave velocities v_{S1} = 250 m/s and v_{S2} = 1000 m/s have been taken from the wave velocity evaluation. The height of the layer H = 10 m has been fitted to the transfer function. The deep stiff (rock) soil yields very low low-frequency amplitudes whereas the thick softer top layer determines the higher amplitudes in the wide range between 10 and 50 Hz. A strong

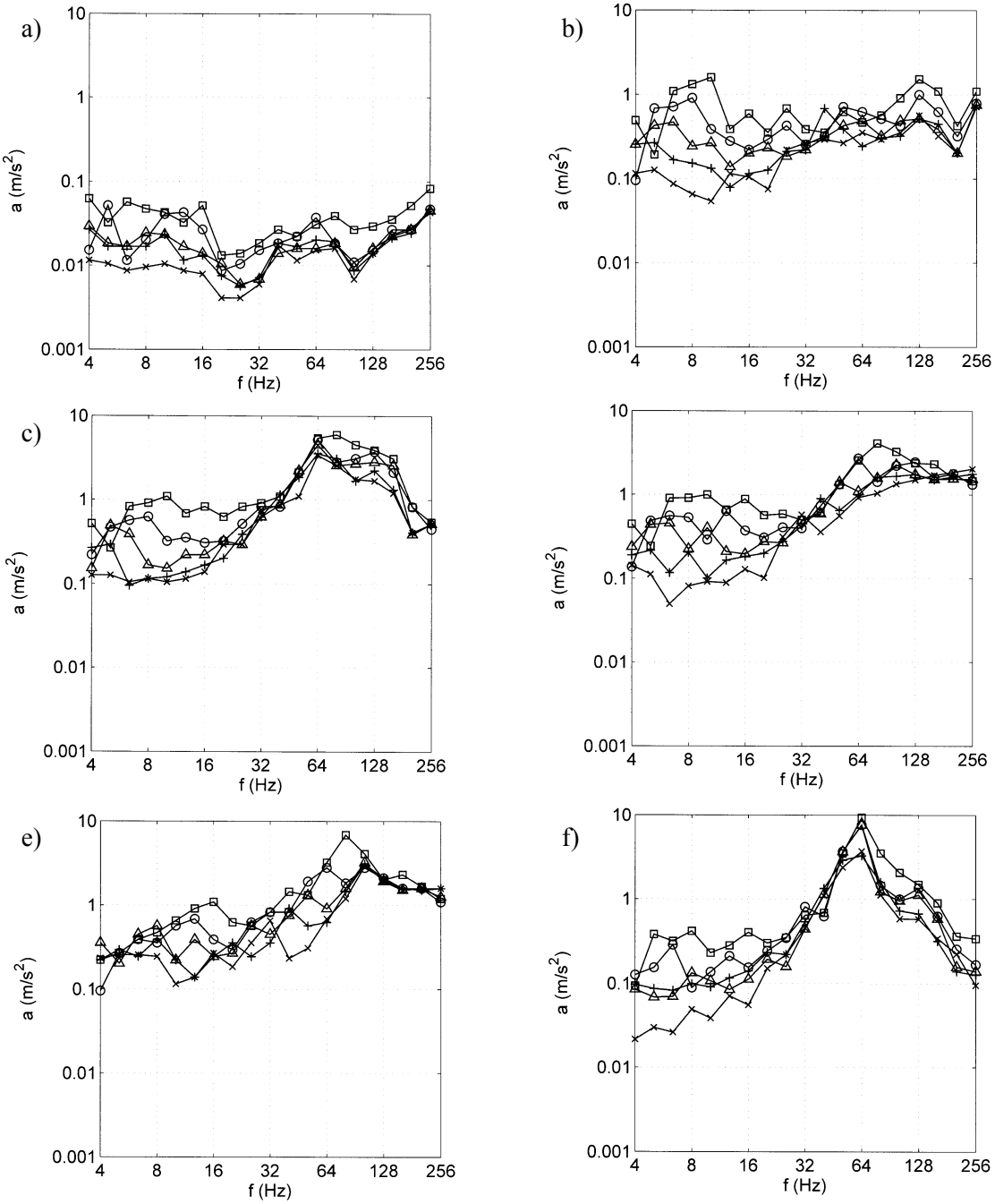

Figure 3. German test site, variable train speed □ 63, ○ 80, △ 100, + 125, × 160 km/h, a) car body, b) bogie, c) wheel 1, d) wheel 2, e) wheel at ballast bridge track, f) wheel at slab track.

reduction at higher frequencies is probably due to the increasing material damping $D(f)$ = 1-10 %.

The train-induced ground vibrations are presented for four different distances in Figures 5a-d, always for the five train speeds v_T = 63, 80, 100, 125, 160 km/h. Close to the track at r = 2.5 m (Fig. 5a), the sleeper passage can be found at 32, 40, 50, 63 and 80 Hz. The quasi-static component due to the passage of the static load is also present in the low-frequency near-field of the higher train speeds (at 4 to 6 Hz for 100 to 160 km/h). At longer distances (Fig. 5b), the quasi-static component has disappeared and the low frequency amplitudes are small. The high-frequency amplitudes above 64 or 80 Hz are also reduced strongly. Two frequency ranges around 12 and 50 Hz can be distinguished at Figure 5b and 5c.

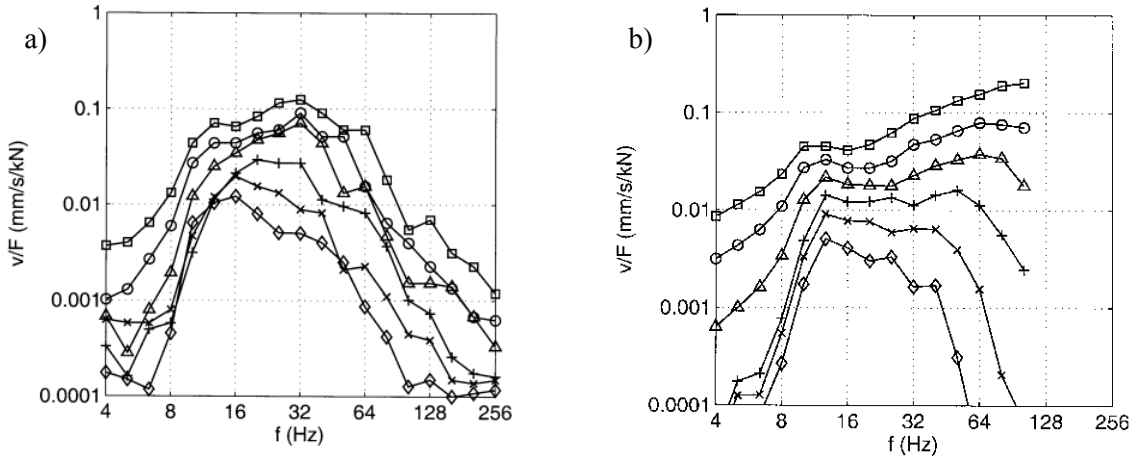

Figure 4. German test site, transfer function of the soil a) measured, □ 2.5, ○ 7.5, △ 12.5, + 22.5, × 37.5, ◇ 62.5 m, b) theoretical model □ 2,○ 4, △ 8, + 16, × 32, ◇ 64 m.

They are equally strong at mid distance (Fig. 5b), but the first maximum becomes stronger at long distances (Fig. 5c). At the far-field (Fig. 5d), only the first frequency range is still present.

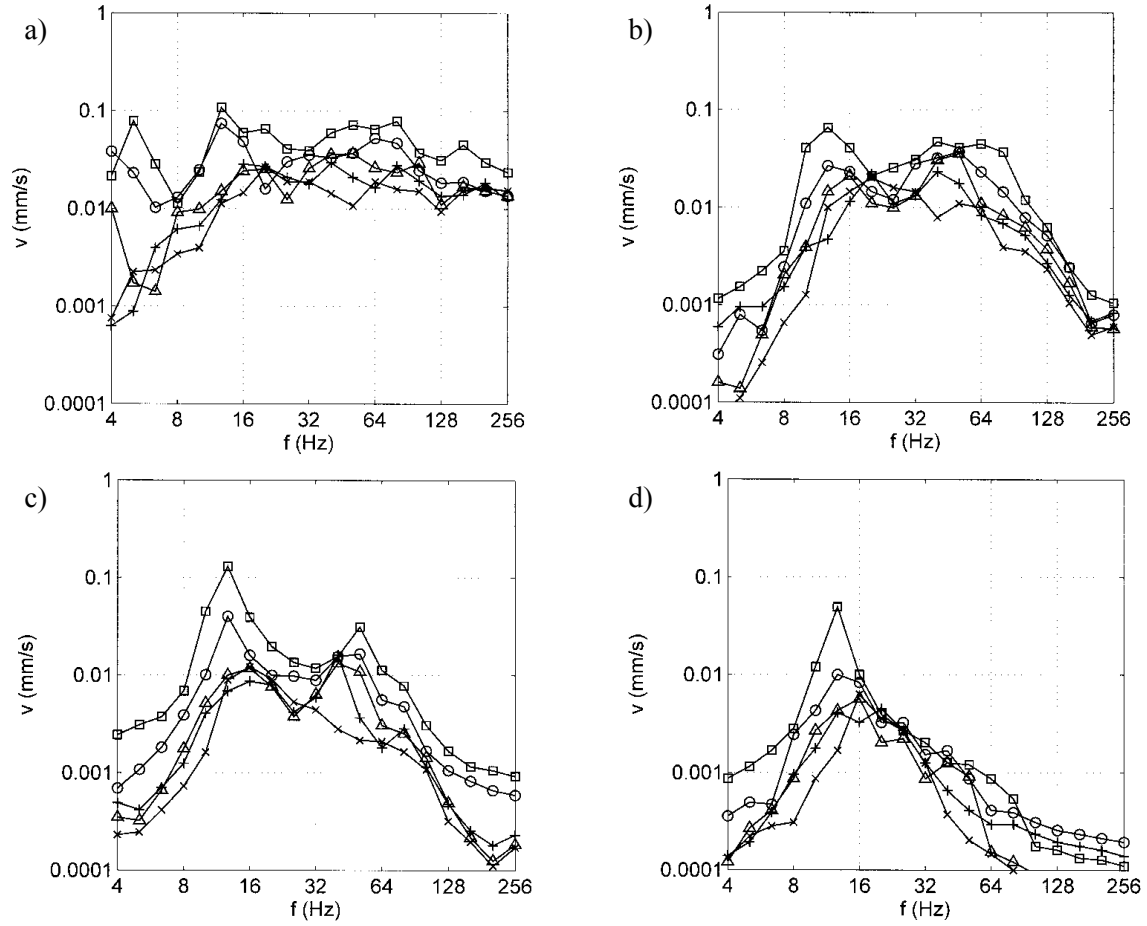

Figure 5. German test site, train-induced ground vibration for variable train speed × 63, + 80, △ 100, ○ 125, □ 160 km/h, a) at 2.5, b) 17.5, c) 30, and d) 100 m distance from the track.

4. Measurements at the Swiss sites and the analysis of the excitation forces

A measurement campaign at more than 10 sites has been performed in Switzerland by the Federal Institute of Material Research and Testing (BAM) where hammer- and train-induced vibrations have

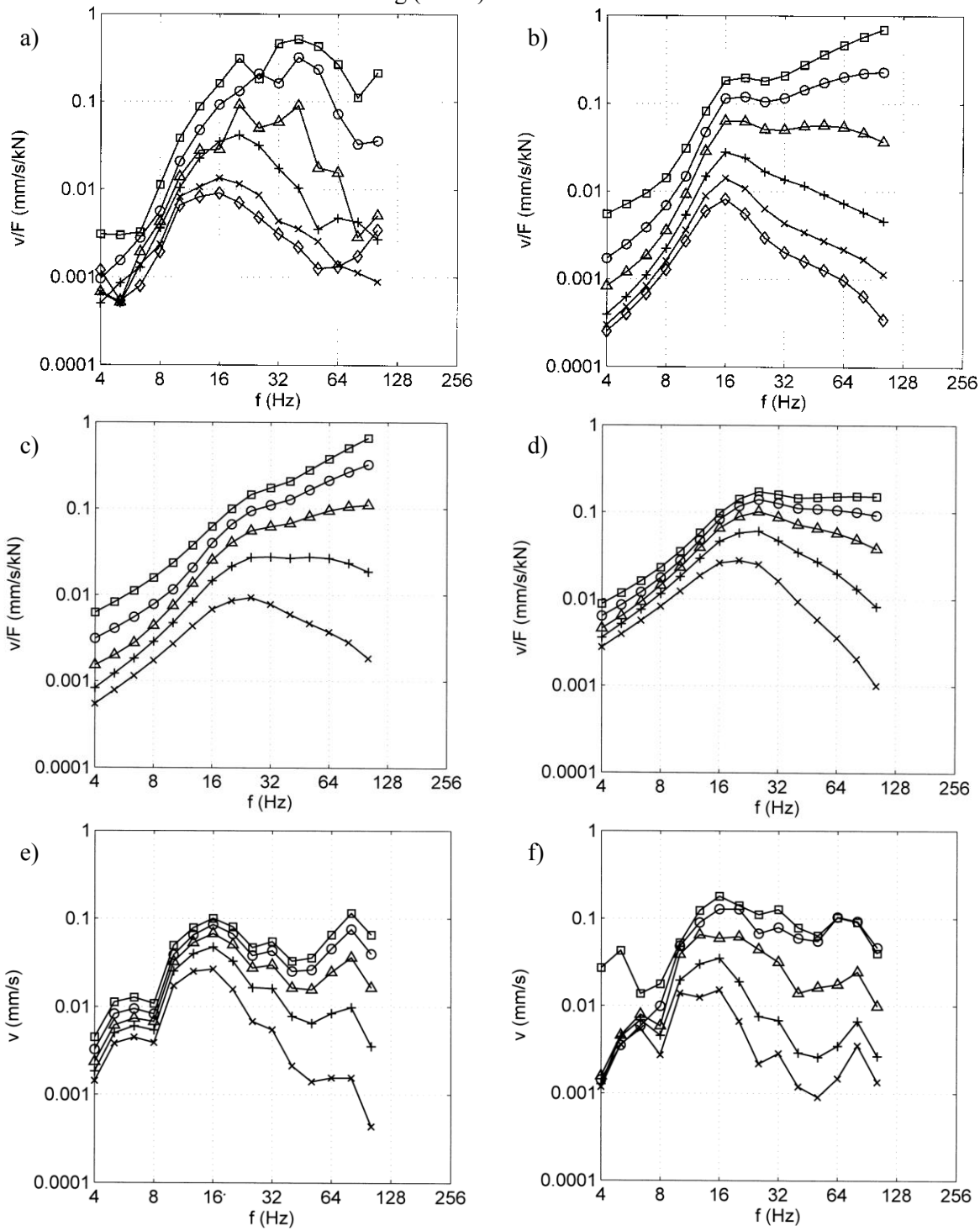

Figure 6. Swiss test site, prediction scheme, a) measured transfer function of the soil, b,c) calculated transfer functions of the soil, b) from measured transfer function, c) from wave velocity measurements, d) calculated transfer function train, e) prediction with specific load spectrum, f) measured train-induced vibration, distances $r \approx$ □ 4, ○ 8, △ 16, + 32, × 64 m.

been measured [18]. At some of these sites, the Swiss Railways (SBB) have done axle-box measurements [19] which have been evaluated also by BAM.

4.1. Hammer excitation, transfer function train, and the prediction of train induced ground vibration
The experimental and theoretical prediction procedure is presented for one Swiss site in Figure 6. The hammer impact measurement is evaluated to estimate the frequency-dependent wave velocity (dispersion) or the transfer function (of a point load, the hammer excitation Fig. 6a, [17]). Many layered soil models are calculated and the best fit either to the dispersion curve (Fig. 6c, v_{S1} = 150 m/s, v_{S2} = 250 m/s, H = 3.5 m, D = 2 %) or to the transfer function (Fig. 6b) is used for the further calculation. Note that both approximations differ only in details whereas low- and high-frequency levels are almost the same. Many point-load transfer functions have been superposed to get the transfer function of a train (Fig. 6d). The effect of the load distribution across the track (Fig. 1) can be clearly found at the reduced high-frequency amplitudes of Figure 6d compared to Figure 6c. The transfer function (Fig. 6d) can be read as the response to a train excitation of 1 kN per axle and third of octave which is already a good approximation. A more specific force spectrum is calculated from the measurements and used for a prediction (Fig. 6e). The prediction is quite similar to the measured train-induced ground vibration (Fig. 6f) and thus validating the transmission (wave propagation) part of the prediction procedure. Note that the transfer function train (Fig.6d) can also be used for a back-calculation of the excitation force from the measured ground vibration.

4.2. Excitation forces from axle-box measurements and back-calculated from ground vibrations
Some results of axle-box measurements are shown in Figure 7. The accelerations of four wheels of the measurement car passing at the Swiss site are quite similar (Fig. 7a). The general trend is the same as at the German site (Fig. 3c,d), constant low low-frequency amplitudes and high high-frequency amplitudes. The results of four wheels have been averaged and are presented for seven sites in Switzerland in Figure 7b. All axle-box accelerations display the same trend and the amplitudes are the same as at the German site, 1 m/s^2 or lower at low frequencies or 3 m/s^2 or higher at high frequencies.

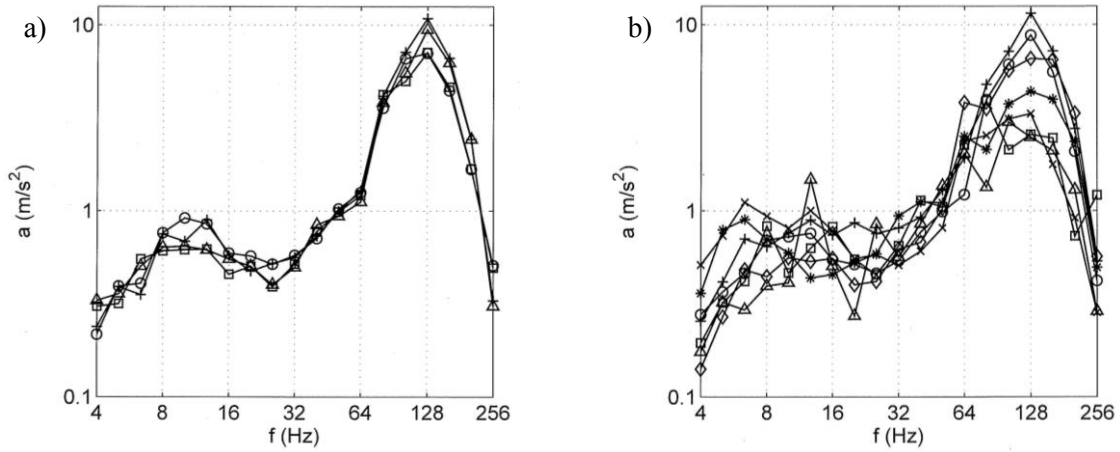

Figure 7. Swiss test site, axle-box measurements, a) 4 wheels at site 1, b) 4 wheels averaged at seven different Swiss sites, ○ site 1.

A nominal excitation force per wheelset can be calculated by multiplying the measured acceleration by the mass of the wheelset (1500 kg, Fig. 8a). On the other hand, excitation forces can be back-calculated from the measured ground vibration using the train transfer functions of each site (e.g. Fig. 6d, [14]). The resulting forces in Figure 8b have approximately the same level of 1 kN per wheelset and third of octave. This confirms the methods of analysis. Nevertheless, some deviations have been found and will be discussed in Section 6. Some low-frequency force amplitudes are higher for the ground vibration measurements and most high-frequency forces are higher for the axle-box measurements.

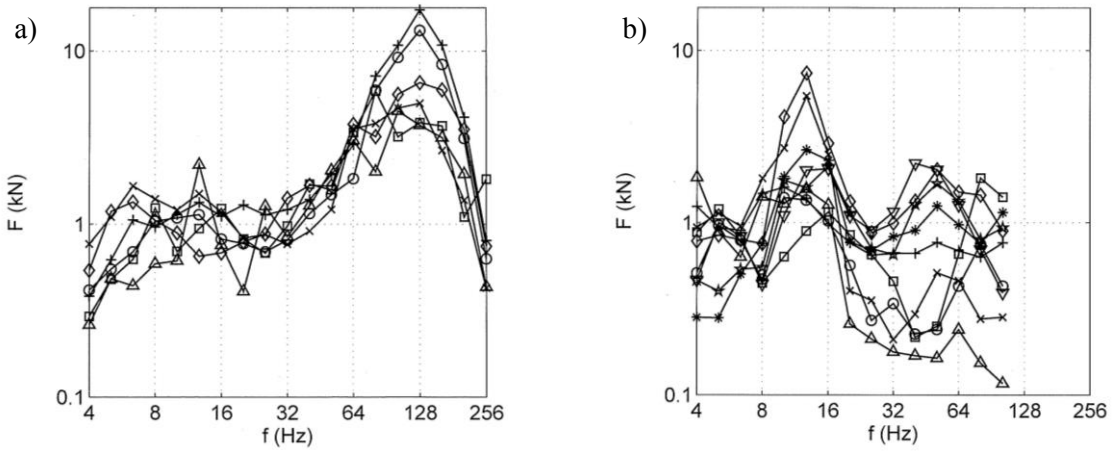

Figure 8. Excitation forces from a) measured axle box accelerations at six Swiss sites, ○ site 1 and b) from measured ground vibrations at different Swiss sites □, △, +, ×, ○ site 1, and different German sites ✳, ▽, ☆, ◇ site G1.

5. Measurements at the French site and the vehicle-track-soil calculations for France and Germany

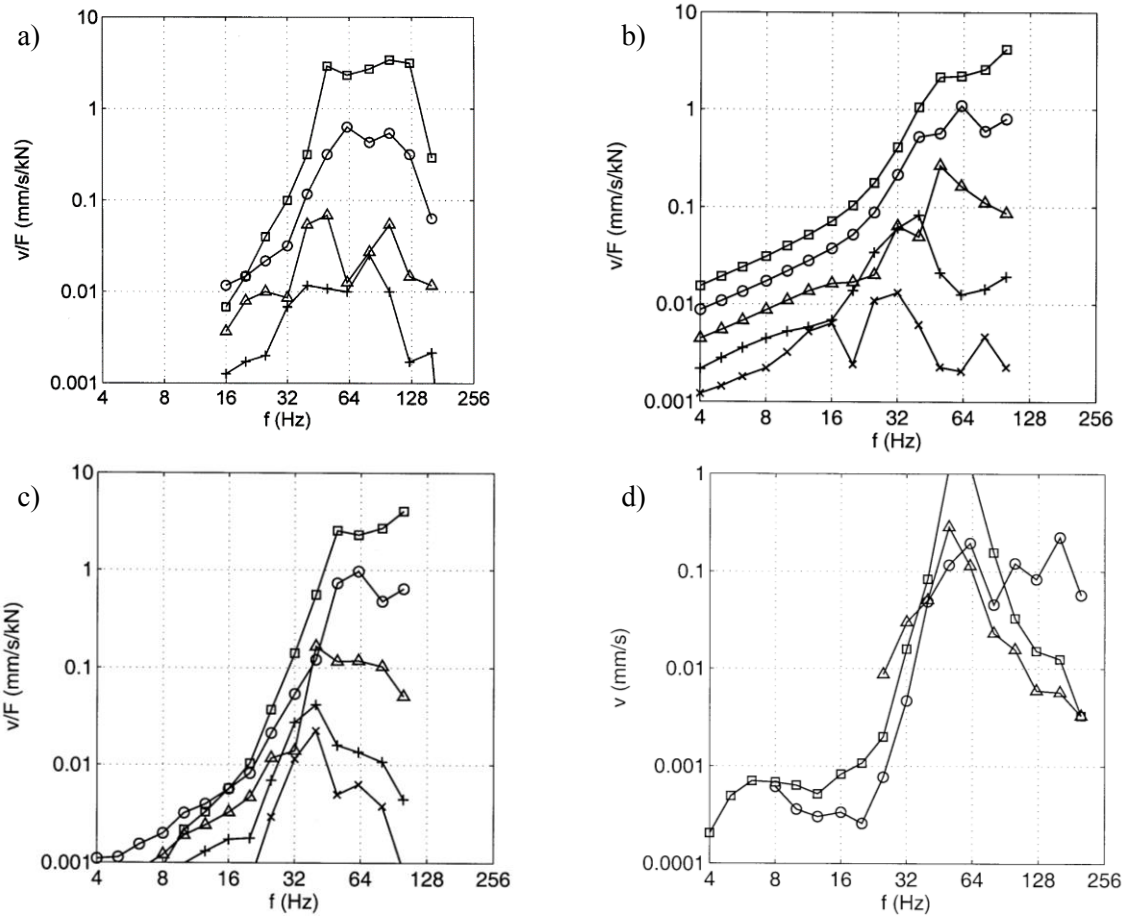

Figure 9. French test site, transfer function of the soil a) measured, b) theoretical model from wave velocity measurements, c) theoretical model from transfer function measurements, □ 2,○ 4, △ 8, + 16, × 32 m, tram-induced ground vibration, v_T = 40 km/h, r = 2 m, △ measurements, □ calculation, ○ calculated with the measured transfer function.

Ecole Centrale de Nantes has made several measurements in cooperation with INRETS Lyon (Ifsttar) at four tramway lines in Nantes [5,20]. The results for the line on a slab track will be presented here.

5.1. Ground vibration measurements for hammer and tramway excitation

As for the other sites, the soil at the French site has been analysed by hammer excitation. The measured transfer function is shown in Figure 9a. The high high-frequency amplitudes indicate a soft top soil whereas the low low-frequency amplitudes indicate a stiff underlying soil. The soil model from the wave velocity analysis consists of three layers of v_{S1} = 77 m/s and H_1 = 0.4 m, v_{S2} = 111 m/s and H_2 = 0.6 m, and v_{S3} = 208 m/s (half-space). The top layers have a strong material damping of D = 7.5 and 5 %. The corresponding transfer functions are presented in Figure 9b. To get a better approximation of the low low-frequency amplitudes of the measured transfer functions, a second model has been developed (Fig. 9c) which has a stiffer half-space of v_{S4} = 500 m/s under the third layer of H_3 = 0.5 m. The tramway-induced ground vibrations are shown in Figure 9d. The strong increase between the low- and high-frequency amplitudes from the hammer measurement can also be found for the tramway-induced vibrations.

5.2. Measurements and calculations for the vehicle-track-soil interaction

The irregularities have been determined twofold. The irregularities of the track have been measured directly in the range of wavelengths of 0.1 to 1.2 m. The combined vehicle and track errors s can be evaluated from the wheelset accelerations a as $s = a/(2\pi f)^2$. Both results have been used to define the combined and simplified irregularities of vehicle and track (Fig. 10a). The respective irregularities of the German site are given for comparison. The irregularities in the common wavelength range are quite similar. This range is sufficient for the urban traffic in Nantes. For the higher speeds of the intercity traffic, the longer wavelengths are also of interest which have a stronger increase with wavelength than the short wavelengths. Whereas the irregularities are unique functions $s(\lambda)$ of the wavelength, the irregularity spectra $s(f)$ must be calculated dependent of the train speed as $s(f) = s(\lambda = v_T/f)$. The results for the tramway with v_T = 40 km/h and the passenger train with v_T = 160 km/h are shown in Figure 10b. The irregularities are decreasing with frequency.

Figure 10b shows also the vehicle-track transfer functions $H_{VT}(f)$ between the irregularities and the excitation forces acting on the track. These transfer function are increasing with $H_{VT} \sim f^2$ until the vehicle-track resonance at 64 resp. 100 Hz. For higher frequencies the transfer function remains constant or decreases for the track in Nantes. The differences between Nantes and Würzburg are typical for a slab track and a ballast track (see also Fig. 3d,f). The slab track in Nantes has softer rail pads, therefore a lower resonance frequency and, due to the weak material damping, a higher resonance amplitude.

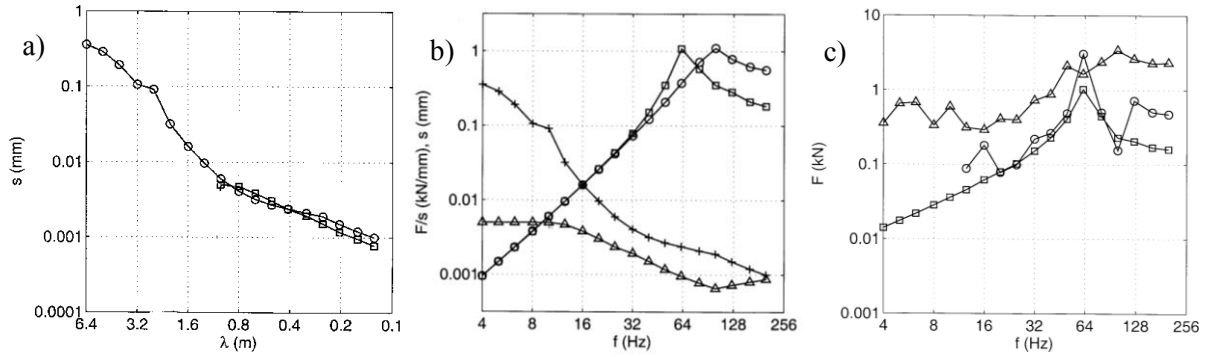

Figure 10. French and German test site a) vehicle and track irregularities (combined and simplified) ☐ F, ○ G, b) irregularity spectra for △ 40 km/h F and ＋ 100 km/h G, transfer functions F/s ☐ F, ○ G, c) excitation forces ☐ F calculated,○ F and △ G from measured wheelset accelerations

The excitation forces F can then be obtained from the irregularities s and the vehicle-track transfer function H_{VT}. The excitation forces at the sites of Nantes are weakly increasing with frequency until the strong resonance at 64 Hz (Fig. 10c). After the resonance, the force amplitudes are decreasing. The excitation forces can also be estimated from the axle-box measurements. The results from axle-box measurements and from irregularity-based calculations are quite similar except for the very high frequency amplitudes. The discrepancy for the high-frequency forces has been thoroughly analysed in [5]. A rotational wheelset-track resonance at 120 Hz has been found in addition to the vertical wheelset-track resonance at 64 Hz. Moreover, the antimetric response is dominant in the whole high-frequency range between 80 and 200 Hz. The measurements at the other three sites in Nantes have shown the same wheelset behaviour. At the German site, the decrease of the irregularities and the increase of the transfer function compensate for almost constant excitation forces around 1 kN.

Finally, the ground vibration near the track can be predicted by using the excitation forces and the transfer function of the soil (Fig. 9d), where both, the measured and the calculated transfer functions have been used successfully at the French site. A similar good agreement between measured and predicted ground vibrations has been achieved for the German site (Fig. 11). Once again, little higher high-frequency amplitudes have been predicted based on the axle-box measurements.

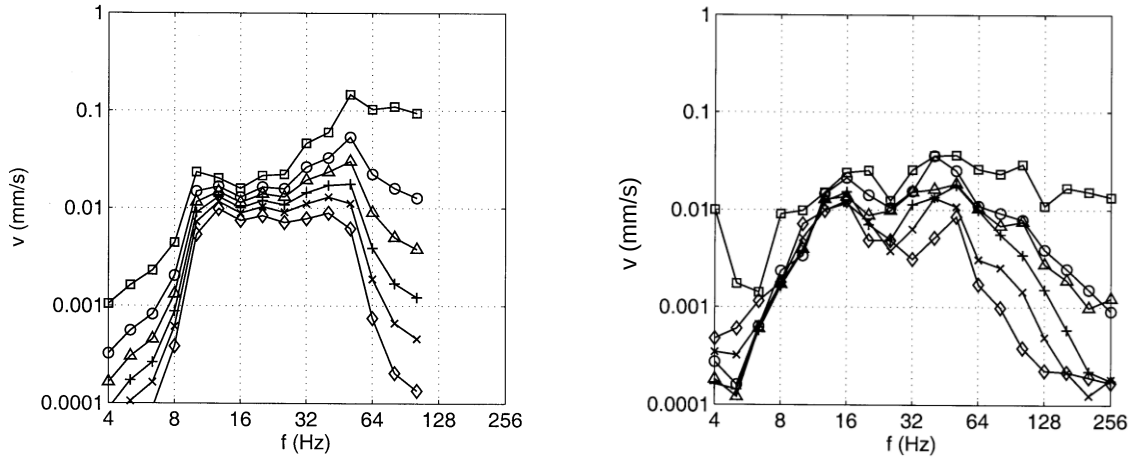

Figure 11. German test site, train-induced ground vibrations, v_T = 100 km/h, a) prediction, b) measurement, distances □ 2.5, ○ 7.5, △ 12.5, + 20, × 30, ◇ 50 m.

6. Discussion

The various experimental and theoretical results confirm that the excitation and propagation of train-induced ground vibration are well understood. Nevertheless, the observed deviations which are similar for several sites should be discussed.

6.1. High-frequency axle-box measurements

It has been found that the axle-box measurements yield higher high-frequency amplitudes than expected from the ground vibration measurements and from the theory. One reason has been found in the

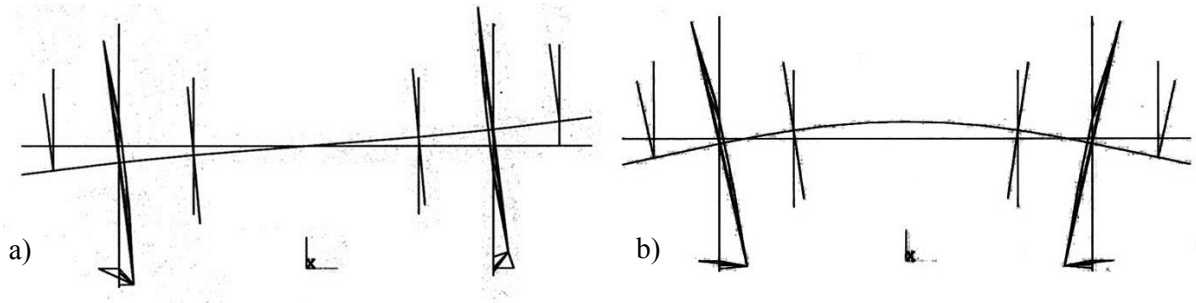

Figure 12. Non-uniform vibration modes of the wheelset, a) rotational mode, b) elastic mode.

antimetric response of the wheelset [5] which yields high amplitudes for the axle-box acceleration but only small amplitudes for the resulting excitation force. Moreover, an elastic eigenmode of the wheelset lies in the same high-frequency region. This mode cannot produce any significant excitation force. Figure 12 shows the rotational and elastic wheelset modes. Due to this behaviour, the axle-box acceleration can only be used up to the first vertical resonance. For higher frequencies, multiplying the whole wheelset mass and the axle-box acceleration highly overestimates the excitation force. A similar idea has been followed in [21].

6.2. Low-frequency ground vibrations

The measured excitation forces cannot generate a certain low-frequency ground-vibration component at several sites. This frequency range depends on the train speed and lies between 8 and 16 Hz for the inter-city passenger trains. It can also be found for high-speed trains where two examples from Portugal (16 to 25 Hz for v_T = 212 km/h) and Spain (20 to 32 Hz for v_T = 300 km/h) are given in Figure 13. For urban traffic with low speeds, this vibration component has very low frequencies and low amplitudes and no importance. The observed spectrum is at the high end of the axle-impulse spectra which occur for the passage of the static loads over the track. These axle impulses regularly superpose to produce the quasi-static response of the near-field soil. If the soil is not regular but has some random stiffness variation, a scattered part of the axle-impulses will be found also at far-field points [22]. The scattered axle impulses in a randomly heterogeneous soil are an important conclusion of the parallel vehicle, track and soil measurements.

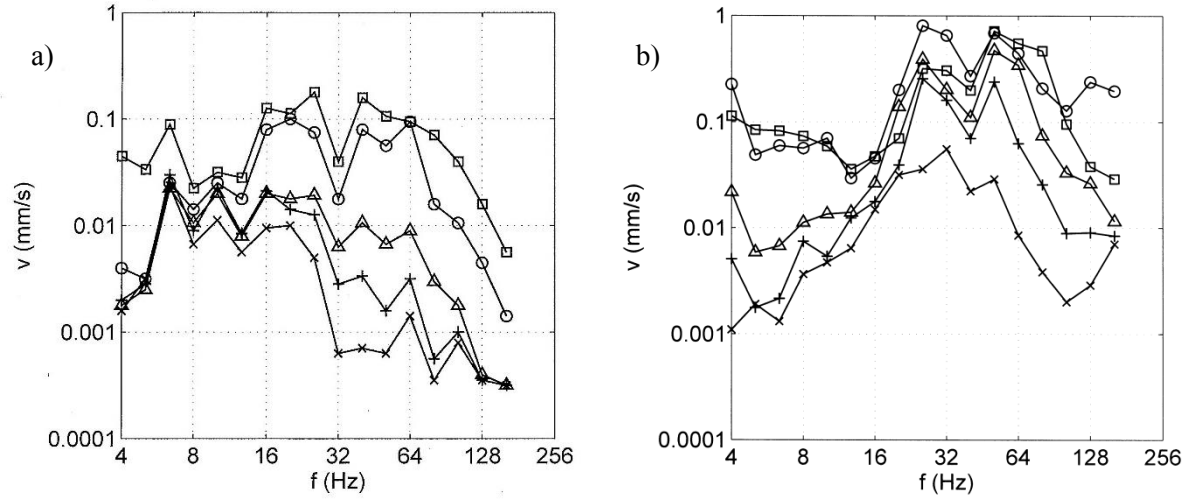

Figure 13. High-speed train-induced ground vibration in Portugal after [6], r = □ 3.5, ○ 7, △ 15, + 30, × 45 m, and Spain after [7], r = □ 3, ○ 9, △ 12, + 15, × 32 m.

7. Conclusions

Vehicle, track and soil measurements have been performed at the sites in Germany, Switzerland and France. The comparison of these measurements with each other and with theory confirms the correct prediction of train-induced vibrations. Besides the good correlation between irregularities of the vehicle and track, the accelerations of the wheelset, the excitation forces and the ground vibration amplitudes, two minor deviations have been found. There are an additional low-frequency ground vibration component, which is attributed to the scattering of axle impulses in a randomly heterogeneous soil, and additional high-frequency vibration components of the wheelsets. A wheelset has high-frequency rotational and elastic modes which produce only minor ground vibrations.

Acknowledgements

Thanks to all who participated in the measurements, namely, S. Said, W. Schmid, W. Wuttke, F. Ziegler. Thanks for the good cooperation to H. Grütz (DB), R. Müller (SBB), and M. Maldonado (EC Nantes).

References

[1] Fryba L 1972 *Vibrations of Structures under Moving Loads* (Groningen: Noordhof Int. Publishing)
[2] Knothe K and Grassie S 1993 Modelling of railway track and vehicle/track interaction at high frequencies *Vehicle System Dynamics* **22** 209-262
[3] Madshus C and Kaynia A 2000 High speed railway lines on soft ground, dynamic behaviour at critical speed *Journal of Sound and Vibration* **231** 689-701
[4] Sheng X 2001 *Ground vibration generated from trains* (PhD Thesis, Southampton: University of Southampton)
[5] Maldonado M 2009 *Vibrations dues au passage d'un tramway – mesures expérimentales et simulations numériques.* (PhD Thesis, Nantes: Ecole Centrale de Nantes)
[6] Alves Costa P 2011 *Vibrações do sistema via-maciço induzidas por tráfego ferroviário - modelação numérica e validação experimental.* (PhD Thesis, Porto: University of Porto)
[7] Romero A 2012 *Predicción, medida experimental y evaluación de las vibraciones producidas por el tráfico ferroviario* (PhD Thesis, Sevilla: University of Sevilla)
[8] Degrande G and Schillemanns L 2001 Free field vibrations during the passage of a Thalys high-speed train at variable speed *Journal of Sound and Vibration* **247** 131-144
[9] Zhai W, Wei K, Song X, and Shao M 2015 Experimental investigation into ground vibrations induced by very high speed trains on a non-ballasted track. *Soil Dynamics and Earthquake Engineering* **72** 24-36
[10] Feng S, Zhang X, Wang L, Zheng Q, Du F, and Wang Z 2017 In situ experimental study on high-speed train induced ground vibrations with the ballastless track. *Soil Dynamics and Earthquake Engineering* **102** 195-214
[11] Kausel E and Roesset J 1981 Stiffness matrices for layered soils *Bulletin of the Seismological Society of America* **71** 1743-1761
[12] Wolf J 1985 *Dynamic Soil-Structure Interaction*, (Englewood Cliffs, New Jersey: Prentice-Hall)
[13] Auersch L 1994 Wave propagation in layered soil: theoretical solution in wavenumber domain and experimental results of hammer and railway traffic excitation *Journal of Sound and Vibration* **173** 233-264
[14] Auersch L 2010 Theoretical and experimental excitation force spectra for railway induced ground vibration – vehicle-track soil interaction, irregularities and soil measurements. *Vehicle System Dynamics* **48** 235-261
[15] Auersch L, Said S and Rücker W 2001 *Das Fahrzeug-Fahrweg-Verhalten und die Umgebungs-erschütterungen bei Eisenbahnen* (Forschungsbericht 243, Berlin: BAM)
[16] Zakel H and Willenbrink L 1997, *Körperschallmessungen an einem Bm 235-Wagen bei der Fahrt auf verschiedenen Oberbauten der Neubaustrecke Fulda-Würzburg* (Report to BAM, München: Deutsche Bahn AG Forschungs- und Technologiezentrum)
[17] Auersch L and Said S 2015 Comparison of different dispersion evaluation methods and a case history with the inversion to a soil model, related admittance functions, and the prediction of train induced ground vibration *Journal of Near Surface Geophysics* **13** 127-142
[18] Said S, Wuttke W, Ziegler F and Peuschel M 2014 *Messung von Zugerschütterungen und Boden-kennswerten an Trassen der Schweizerischen Bundesbahn – Messort Selzach* (Interner Mess-bericht, Berlin: BAM)
[19] Dutoit P 2016 *Intercity-Neigezug und Reisezugwagen, Spezialmessung vertikale Beschleunigun-gen an Achsbüchsen* (Bericht, Bern: SBB)
[20] Maldonado M, Chiello O et al. 2009 *Bruit et vibrations dus aux tramways: émission et perception* (Rapport 279, Lyon: INRETS)
[21] Ntotsios E, Thompson D and Hussein M 2017 The effect of track load correlation on ground borne vibration from railways *Journal of Sound and Vibration* **402** 142-163
[22] Auersch L 2006 Ground vibration due to railway traffic – The calculation of the effects of moving static loads and their experimental verification *Journal of Sound and Vibration* **293** 599-610